

Fluctuations in Number of Water Molecules Confined between Nanoparticles

Changsun Eun and Max L. Berkowitz*

Department of Chemistry, University of North Carolina, Chapel Hill, North Carolina 27599, United States

Received: August 2, 2010; Revised Manuscript Received: September 15, 2010

We used molecular dynamics computer simulations to study the character of interactions between two nanoscale graphene plates in water and also between plates made of “carbon” atoms that have different interaction strength with water. Fluctuations in the number of water molecules in the confined space between plates are qualitatively similar when the plates are made of graphene or when the plates contain “carbon” atoms with weaker “carbon”–water interaction strength. We also observed that these fluctuations are strongly enhanced compared to the fluctuations observed next to a single plate. If the character of water fluctuations in the confined space determines the character of interactions, then it is possible to conclude that the interaction between graphene plates in water is hydrophobic.

Introduction

A while ago it was suggested that, while the hydrogen bonding in water around a small hydrophobic region is maintained, it is disrupted around a large hydrophobic region.¹ Recent studies^{2–11} of the hydrophobicity effect demonstrated that, indeed, its manifestations including hydrophobic hydration and hydrophobic interactions depend on the sizes of hydrophobic solute particles. If the size of the solute is small, so that the hydrogen bonds around the solute are not significantly disrupted, one can use information theory and scaled particle ideas to model hydrophobic hydrations and interactions.^{2,3,6,12} In this case, the solvation free energy of the solute is proportional to the solute volume and the hydrophobic interaction is determined by the entropic component. When the size of hydrophobic particles is substantially large, so that the particle disrupts the water hydrogen bonding network, the hydration free energy is proportional to the area of the particle and the hydrophobic interaction free energy is dominated by the enthalpic component.^{4,10,13} The crossover from one regime to the other occurs at a certain particle size and it strongly depends on pressure and temperature of the system: it is around 1 nm at ambient conditions.^{14,15} Whereas the small-scale solute hydration is explained by mostly considering statistical properties of cavities in bulk water,³ the large-scale solute hydration is explained by the change in the properties of the particle–water interface.⁴ In cases when the larger solute–water interaction is strongly dominated by a hard-core repulsion, the number of water molecules at the interface is reduced and the interface is similar to the one between water and its vapor; dewetting occurs next to the particle and it can be seen by inspecting the average water density at the interface.¹⁶ If the strength of the attractive force acting between the larger scale particle and water increases, the average water density at the interface also increases and the surface of the particle is becoming wet. Nevertheless, the character of fluctuations in the number of water molecules in a volume next to the surface is different from the character of fluctuations in the same volume of bulk water.^{16–18} In bulk water and next to hydrophilic surfaces, the fluctuations have a Gaussian character, whereas next to hydrophobic surfaces these fluctuations display a fat tail toward a small number of water molecules,¹⁷ pointing out that it is easier to create cavities at the interface and that the interface is softer. The increased ability

to create cavities at the water interface was previously demonstrated in simulations that studied water/nonpolar liquid interfaces.¹⁹ The softness of the water/hydrophobic particle interface can be also measured by the magnitude of the second moment of fluctuations,²⁰ which is proportional to the compressibility when the probing volume is very large. Therefore, it was proposed that the presence of large fluctuations in the number of water molecules at the interface can serve as a signature of a *hydrophobic hydration* of the particle.²⁰ Can the same criterion, related to the fluctuation in number of water molecules, be used to study the phenomenon of *hydrophobic interaction* when two nanoscale particles approach each other in water?

To determine if the interaction between small-scale particles is hydrophobic, one can study the behavior of different properties relevant to the interactions, such as osmotic virial coefficients and its temperature dependence, although they provide an indirect way to understand the solvent structure near apolar solutes and also are very sensitive to the details of the effective solute–solute interaction at large separations.²¹ But, perhaps, the simplest and the most intuitively appealing definition of the hydrophobic interaction follows from considering the work (free energy change), $\Delta G(R)$, of bringing two particles from an infinite separation to a distance R between fixed locations in particles, like their centers of mass. If $\Delta G(R)$ in water has a notably deeper minimum at distance $R \approx \sigma$ (σ is the diameter of the solute) than the minimum in other solvents, the interaction can be considered to be hydrophobic.²² To eliminate the effect of direct interaction between particles, one subtracts the potential of interaction between particles from the total work, and obtains a quantity that measures the effect of the solvent on interaction, that is

$$\delta G(R) = \Delta G(R) - U(R) \quad (1)$$

Therefore, one can define hydrophobic interaction as the interaction that results in a condition that $\delta G(\sigma) < 0$. It is also possible to adopt the same definition of hydrophobic interaction to the case of larger scale particles, assuming that R is the distance between surfaces, which is well defined when, for example, we consider interaction between rigid model surfaces such as graphene plates. To study possible hydrophobic interaction between two graphene plates, Choudhury and Pettitt⁵

calculated the potential of mean force between these plates interacting in water. The simulations showed that δG was positive at a large range of distances R including distance $R = \sigma$, thus indicating that the interaction between graphene plates is not hydrophobic, according to the definition given above that uses eq 1. It is interesting that the value of $\delta G(\sigma)$ allows the determination of the surface tension and therefore the hydration character of the plate. δG , the solvation part of the free energy, is equal to $4\gamma_{ws}A$ when two plates are at infinite separation (because four surfaces are solvated) and it is equal to $2\gamma_{ws}A$ when the surfaces are at distance σ in their contact, where A is the area of the plate and γ_{ws} is the water–solid plate surface tension. The difference in these free energies, which is $\delta G(\sigma)$, is equal to $-2\gamma_{ws}A$. From this result we conclude that γ_{ws} is negative, because $\delta G(\sigma) > 0$, and therefore the graphene plates are hydrophilic. The hydrophobic (or hydrophilic) character of a graphene or any other surface can be also determined by considering the angle that a water droplet makes with a surface, but as was pointed out, this is very hard to do when the particle is nanoscopic in size.¹⁸ In this case it was shown that the hydrophobic character of a surface can be determined by the fluctuation character of water next to the surface and that next to hydrophobic surfaces the fluctuations in number of water molecules are large.¹⁸ To follow up on this idea, we decided to check if the fluctuations in the number of water molecules between surfaces can determine the character of the *interaction* between such surfaces, that is, determine if the interaction is hydrophobic or hydrophilic.

Therefore, we studied the potential of mean force (PMF) between two graphene plates immersed in water and compared it to the PMF between two plates with strongly reduced “carbon”–water interaction, so that the plates have a hydrophobic character.

Methods

To calculate the PMFs and changes in the fluctuations of water molecules in the confined space between the plates, we performed molecular dynamics (MD) simulations on seven different systems. In every system, we considered two plates of size 1.09 nm \times 1.12 nm consisting of 60 “carbon” atoms in hexagonal arrangement immersed in a bath of water containing 1800 water molecules. This size of the plates was chosen to be identical with the size used in the simulation from ref 5 so that we can perform a comparison with that work. A choice of larger-sized plates would be more desirable but would require much larger simulation effort due to the need to increase substantially the number of water molecules in the simulations. We calculated the potential of mean force (PMF or $\Delta G(R)$) acting between plates as a function of the interplate distance, R . To calculate the PMF we followed the procedure described in the article by Choudhury and Pettitt (CP).⁵ As we already mentioned, one of our seven systems we considered was exactly the system from the CP article: two graphene plates in water. The other system had the same geometric arrangement but differed in the strength of “carbon”–water interaction, described by the Lennard–Jones potential. To modify the strength of this interaction, we followed the strategy adopted in another work of CP²³ and modified the strength of the “carbon”–“carbon” interaction parameter, ϵ_{cc} . Because the value of the “carbon”–water interaction parameter is obtained by using the Lorentz–Berthelot combination rule $\epsilon_{co} = (\epsilon_{cc}\epsilon_{oo})^{1/2}$, the change in ϵ_{cc} produces a change in ϵ_{co} (notice that the value of ϵ_{oo} , the parameter for water oxygen–water oxygen interaction, remains fixed in all cases). To make it possible to compare our results with the results reported in the

literature, we report the strength of the “carbon”–water interaction parameter in the values of the “carbon”–“carbon” interaction parameter. Thus, for the case of graphene we used the value of $\epsilon_{cc} = 0.3598$ kJ/mol. In six other cases, the strength of “carbon”–water interaction was different: it was stronger than for graphene–water in one case ($\epsilon_{cc} = 1.0$ kJ/mol), in four cases it was weaker ($\epsilon_{cc} = 0.20, 0.15, 0.10$, and 0.05 kJ/mol). For the remaining case, when the potential of “carbon”–water interaction was considered to be purely repulsive, we used the WCA scheme for potential separation²⁴ based on $\epsilon_{cc} = 0.3598$ kJ/mol. For water, we used the SPC/E model.²⁵

In our simulations, we used the NPT ensemble with Nose–Hoover temperature^{26,27} and Parrinello–Rahman pressure²⁸ coupling algorithms for maintaining 298 K and 1 bar. Electrostatic interaction was calculated through the particle mesh Ewald method²⁹ with a cutoff length of 0.9 nm. The same length was used for the van der Waals interaction cutoff. Periodic boundary conditions were employed. For the PMF calculation, we carried out a series of simulations with different interplate distances from 0.3 to 1.4 nm. The system at an interplate distance of 1.4 nm was considered as the reference state in the calculation. The total simulation time for each MD run was 2 ns and the trajectories from 500 ps to 2 ns were used for data analysis. The coordinates were saved every 1 ps and a time step was 2 fs. All MD simulations were carried out using the GROMACS 3.3.1 and 3.3.3 packages.³⁰

Results and Discussion

In part a of Figure 1, we present the plots that show how the free energies $\Delta G(R)$ and $\delta G(R)$, and the plate–plate interaction energy $U(R)$ change as a function of distance between the plates as the strength of the “carbon”–water dispersion interaction changes. We observe that the minimum of all $\Delta G(R)$ is at a distance ~ 0.34 nm, which coincides with the value of $\sigma_{cc} = 0.34$ nm. As one can clearly see from part b of Figure 1, the value at the minimum of $\Delta G(R)$ at $R \approx \sigma$ is smaller than the minimum for $U(R)$ (and correspondingly $\delta G(\sigma) > 0$) in case of graphene plates, when the value for “carbon”–water interaction is relatively high. Therefore, using the criteria based on the sign of the solvent part of the PMF we may conclude that the interaction between graphene plates is not hydrophobic, but weakly hydrophilic. In other cases, when “carbon”–water interaction is weak the criterion based on the sign of $\delta G(R)$ predicts that the interaction between “carbon” plates is hydrophobic. Do the fluctuations in number of water molecules between plates confirm these conclusions about the character of the interaction between plates?

To study the fluctuations in the number of water molecules, in Figure 1a we also present plots for the average number of water molecules ($\langle N(R) \rangle$) in the rectangular space between plates as a function of the interplate distance. We observe that for ϵ_{cc} having values between 1.00 and 0.15 kJ/mol the $\langle N(R) \rangle$ plots display changes in slopes at two different locations. When plates approach each other from a larger distance, the first change in slope occurs in a region when the distance between plates is ~ 0.9 nm. The water density plots (not shown) demonstrate that this happens when two water layers confined between “carbon” surfaces are reduced to one water layer. After that region, no change in slope is observed, and, therefore, the number of water molecules in the confined space remains constant. The next change in slope occurs at distances between 0.59 and 0.67 nm, depending on the strength of attraction between water and “carbon” atoms. This region is followed up by a region where the number of water molecules in the confined space is zero,

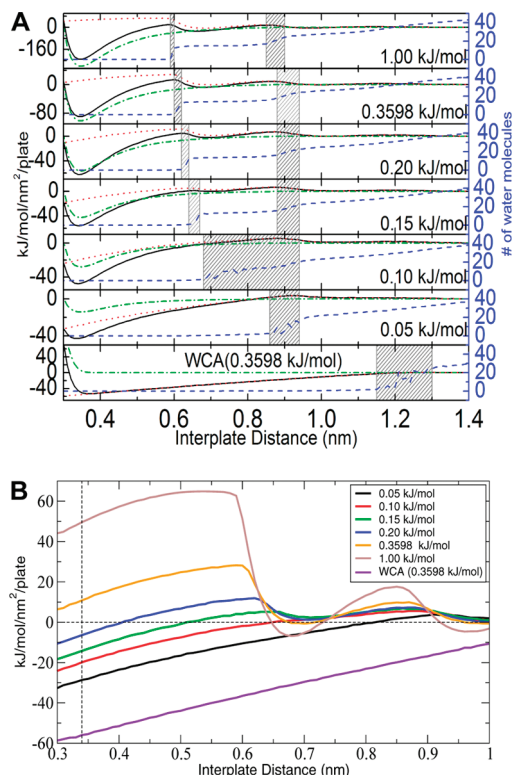


Figure 1. (a) Total PMF $\Delta G(R)$ (black solid line), direct interaction contribution $U(R)$ (green dot-dashed) and water-mediated interaction contribution $\delta G(R)$ (red dotted) as a function of distance between “carbon” plates. Also shown is the average number of water molecules (blue dashed) in the confined space. The numbers in each panel represent ϵ_{cc} . (b) Water-mediated interaction contributions into the PMFs. The vertical line represents $\sigma_{cc} = 0.34$ nm. The PMFs display their minima at $R \approx 0.34$ nm (above figure). The intersection of $\delta G(R)$ curves with the vertical line at 0.34 nm gives the value of the surface tension between the water and the “carbon” surface when the surface is wetted.

corresponding to an absence of water from the space between surfaces; this is consistent with the size restrictions imposed by water and “carbon” atoms, modulated by the presence of attractive interactions between them. The length interval over which the final change in slope occurs is very small. For $\epsilon_{cc} =$

1.0 kJ/mol, the transition from the situation when the space between plates is occupied by water to an empty space is rather abrupt. The length of the transition region broadens, as the attractive interaction decreases to a value of $\epsilon_{cc} = 0.15$ kJ/mol. The observation of water trajectories in the space between plates shows that the disappearance of the last water layer is accompanied by the instability of this layer, that is, large fluctuations in the number of water molecules are present in the intervals around 0.6–0.65 nm. The instability is present for $\epsilon_{cc} = 0.3598, 0.20$, and 0.15 kJ/mol but is absent for $\epsilon_{cc} = 1.00$ kJ/mol. Large fluctuations in the number of waters in the space between plates indicate that this space can be dewetted. Indeed, this can be seen in Figure 2, where we show the number of water molecules between plates as a function of time. We observe that at a certain distance (which depends on the strength of the “carbon”–water interaction) the space is filled up with water or it is empty. From part a of Figure 1 and parts a and b of Figure 2, we observe that qualitative behavior of water molecules in cases with $\epsilon_{cc} = 0.3598, 0.20$, and 0.15 is very similar.

When the value of ϵ_{cc} is reduced to 0.1 kJ/mol, the stable region corresponding to one water layer between plates is not present any more. Once the interplate distance reaches the value of $R \approx 0.9$ nm, the onset of a broad instability region with a width corresponding to the size of a water molecule is observed. Interestingly enough, dewetting for certain time intervals is observed in the interplate space for any value of R belonging to the instability region (part c of Figure 2). When the value of ϵ_{cc} is further reduced to 0.05 kJ/mol, the instability region is narrowed and now corresponds to the location where a transition between two layers to one water layer occurred at higher ϵ_{cc} (like ϵ_{cc} corresponding to graphene plates). For $\epsilon_{cc} = 0.05$ kJ/mol the dewetting is nearly complete when the distance between plates is 0.8 nm, as one can see from part d of Figure 2. In case when the “carbon”–water attractive interaction is absent (this situation is described by WCA repulsive part of the potential), the instability region is pushed further away toward interplate distances in the interval of 1.15 – 1.3 nm, corresponding to distances when three water layers can be found between two graphene plates. Thus we see that strongly hydrophobic surfaces indeed dehydrate the space between them, as can be expected. Comparison between the results obtained for “carbon” plates with WCA potential and plates with $\epsilon_{cc} = 0.05$ kJ/mol shows

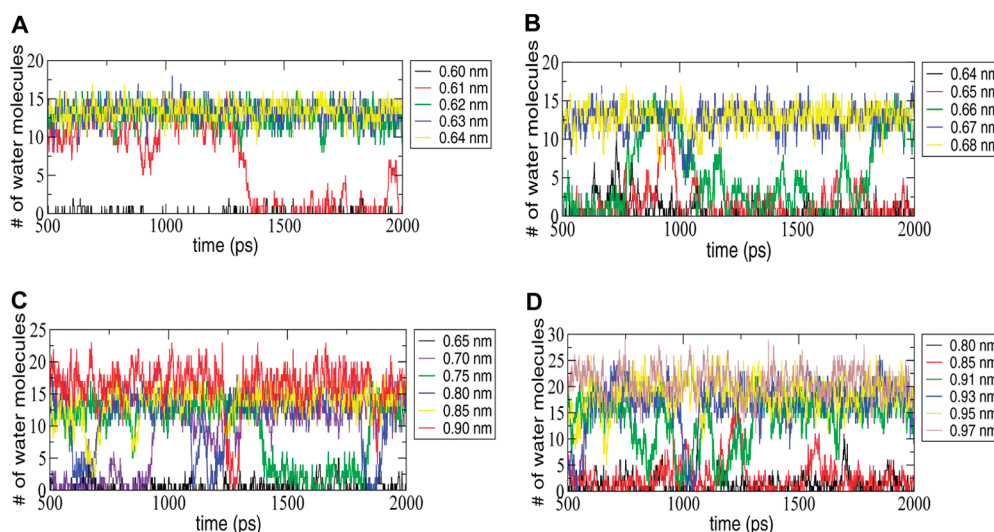


Figure 2. Number of water molecules as a function of time for the cases of $\epsilon_{cc} = 0.3598$ (a), 0.15 (b), 0.10 (c), and 0.05 kJ/mol (d) for different values of the interplate distance.

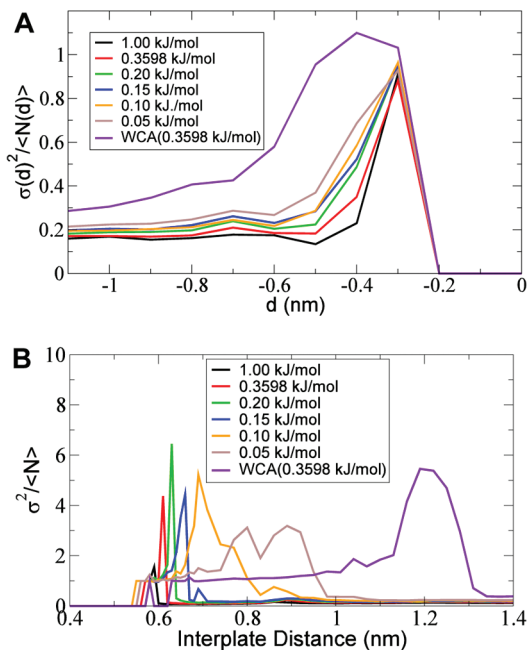


Figure 3. (a) Normalized water number fluctuations in the space next to a single plate for different values of ϵ_{cc} . Negative sign for d indicates that the volume where fluctuations are calculated is on the left side of one of the plates. From the water density profiles we determined that when $d = 0.5$ nm, the probe volume includes the first layer of water molecules next to the plate. (b) Normalized water number fluctuations in the confined space between plates. The numbers in the legend represent ϵ_{cc} values.

that a weak attraction between water and the surface does not eliminate dehydration, only reduces its range. We find that even a relatively strong “carbon”–water interaction, like in case of graphene, does not eliminate dehydration between two graphene plates, although a single graphene plate is hydrophilic.

It was recently suggested that the hydrophobic character of the surface can be determined by the character of fluctuations in the number N of water molecules in the volume adjacent to the surface.¹⁸ Therefore we calculated the variance in these fluctuations, $\sigma^2(N) = \langle N^2 \rangle - \langle N \rangle^2$, next to the surface and, furthermore, in the confined space between two surfaces. Initially, we calculated the values of the variance in the volume next to one plate. These numbers are displayed in part a of Figure 3. Because the volume where we calculate the variance is given by expression $V = Ad$ that is just proportional to distance d from the plate, we present the normalized variance $\sigma^2/\langle N \rangle$ as a function of a distance d . This normalized variance may be also considered as a measure of local water compressibility. As we can see from part a of Figure 3, the character of fluctuations next to the WCA plate differs substantially from

fluctuations in water number next to other plates, thus pointing out the strong hydrophobic character of the WCA plate. The most interesting, of course, is to investigate the fluctuations in the number of water molecules located in the space between plates. We present these calculations in part b of Figure 3, where we show the normalized variance as a function of interplate distance. As we can see from this figure, the values of local compressibility are strongly enhanced in the region. Note that local compressibility values in the instability regions are similar for graphene plates and plates with lower values of $\epsilon_{cc} = 0.20$ or 0.15 kJ/mol.

Conclusions

We present the summary of the results obtained from our seven simulations in Table 1. As we can see the difference in the interpretation of the interaction between plates exists for the case of graphene plates only. If we determine the character of interactions between the plates by the sign of $\delta G(\sigma)$ we need to conclude that graphene plates containing “carbon” atoms with relatively strong attraction between these atoms and water have a hydrophilic character. The calculation of the free energy at contact between plates when ϵ_{cc} is equal or below 0.20 kJ/mol shows that in these cases the plate interaction is hydrophobic. When we consider the fluctuations of water between two “carbon” plates, we observed that the character of these fluctuations is very similar when the plates are graphene or when $\epsilon_{cc} = 0.20$ or 0.15 kJ/mol. Therefore, we may conclude that interaction between graphene plates is hydrophobic.

Why are strong fluctuations in water number present between graphene plates? They are happening due to the collective effect, when the tendency to display fluctuations next to one surface is strongly enhanced as surfaces approach each other. Therefore, two graphene plates, each possibly hydrophilic as a separate plate, can be considered to be engaged in a hydrophobic interaction when approaching each other.

We also carefully searched for the existence of vapor–liquid equilibrium for water in the space between “carbon” plates and observed that it exists even in the case when plates are made of graphene. When the interaction between a “carbon” plate and water is weaker than the interaction between a graphene plate and water, the vapor–liquid equilibrium is easier to observe and it shifts to larger interplate separation distance as the plates are brought together. Clearly, the existence of liquid–vapor equilibrium and presence of large fluctuations in water number between plates are closely related to each other.

We also want to mention that although the systems studied by us are very similar to the systems studied by CP,^{5,23} we reached different conclusions about the behavior of water between graphene plates. In ref 23, CP considered cases when the interplate distance was fixed at a particular value of $R =$

TABLE 1: Summary of the Main Results from Our Simulations Related to the Character of Interaction between “Carbon” Plates in Water and Liquid-Vapor Equilibrium in the Confined Space between the Plates

| ϵ_{cc} (kJ/mol) | water-mediated interaction | | water fluctuations | | |
|--------------------------|----------------------------|--|---|------------------------|--|
| | $\delta G(\sigma)$ | character of interaction based on the sign of $\delta G(\sigma)$ | large water fluctuations at the transition region (two-state equilibrium) | transition region (nm) | character of interaction based on water fluctuations |
| 1.0 | >0 | hydrophilic | no | N/A | hydrophilic |
| 0.3598 | >0 | hydrophilic | yes (1 layer \leftrightarrow 0 layers) | 0.61 | hydrophobic |
| 0.20 | <0 | hydrophobic | yes (1 layer \leftrightarrow 0 layers) | 0.62–0.63 | hydrophobic |
| 0.15 | <0 | hydrophobic | yes (1 layer \leftrightarrow 0 layers) | 0.64–0.67 | hydrophobic |
| 0.10 | <0 | hydrophobic | yes (2 layers \leftrightarrow 0 layers) | 0.68–0.90 | hydrophobic |
| 0.05 | <0 | hydrophobic | yes (2 layers \leftrightarrow 0 layers) | 0.86–0.94 | hydrophobic |
| WCA (0.3598) | <0 | hydrophobic | yes (\sim 2 layers \leftrightarrow 0 layers) | 1.15–1.30 | hydrophobic |

0.68 nm, whereas they changed the strength of “carbon”–water interaction. They concluded that when the interaction strength was such that ε_{cc} was in the region between 0.10 and 0.20 kJ/mol the space between plates was oscillating between dry and wet states. For graphene plates, they concluded that the space between them was wet. In our work, by investigating the transitions over the range of interplate distances, we found that the oscillations between wet and dry states of the interplate region occur also in case of graphene plates, only at slightly smaller separations (part a of Figure 2). This equilibrium between the vapor and liquid states of water in the interplate space between graphene plates is exactly the reason why we may designate the interaction between the plates to be hydrophobic.

Finally, we want to emphasize that hydrophobic phenomena are multifaceted, and all their aspects, perhaps, cannot be adequately considered by one definition. In this article, we demonstrated that using different definitions of hydrophobic interaction we can conclude that interaction between graphene plates may be described either as hydrophobic or as hydrophilic. If the behavior of the fluctuations in water between plates can serve as a more appropriate criterion of the interaction hydrophobicity, we must conclude that graphene interaction in water is hydrophobic.

Acknowledgment. This work was supported by a grant N000141010096 from the Office of Naval Research. We are grateful to Prof. David Chandler for pointing our attention to the connection between surface tension and solvent contribution into the free energy (δG) at the point of plates contact. We also thank the reviewers for their inspiring comments.

References and Notes

- (1) Stillinger, F. H. Structure in Aqueous Solutions of Nonpolar Solutes from the Standpoint of Scaled-Particle Theory. *J. Solution Chem.* **1973**, *2*, 141–158.
- (2) Hummer, G.; Garde, S.; Garcia, A. E.; Paulaitis, M. E.; Pratt, L. R. Hydrophobic Effects on a Molecular Scale. *J. Phys. Chem. B* **1998**, *102* (51), 10469–10482.
- (3) Pratt, L. R. Molecular Theory of Hydrophobic Effects: “She Is Too Mean to Have Her Name Repeated. *Annu. Rev. Phys. Chem.* **2002**, *53*, 409–436.
- (4) Chandler, D. Interfaces and the Driving Force of Hydrophobic Assembly. *Nature* **2005**, *437* (7059), 640–647.
- (5) Choudhury, N.; Pettitt, B. M. On the Mechanism of Hydrophobic Association of Nanoscopic Solutes. *J. Am. Chem. Soc.* **2005**, *127* (10), 3556–3567.
- (6) Ashbaugh, H. S.; Pratt, L. R. Colloquium: Scaled Particle Theory and the Length Scales of Hydrophobicity. *Rev. Mod. Phys.* **2006**, *78* (1), 159–178.
- (7) Janacek, J.; Netz, R. R. Interfacial Water at Hydrophobic and Hydrophilic Surfaces: Depletion Versus Adsorption. *Langmuir* **2007**, *23* (16), 8417–8429.

- (8) Ball, P. Water as an Active Constituent in Cell Biology. *Chem. Rev.* **2008**, *108* (1), 74–108.
- (9) Giovambattista, N.; Lopez, C. F.; Rossky, P. J.; Debenedetti, P. G. Hydrophobicity of Protein Surfaces: Separating Geometry from Chemistry. *Proc. Natl. Acad. Sci. U.S.A.* **2008**, *105* (7), 2274–2279.
- (10) Berne, B. J.; Weeks, J. D.; Zhou, R. H. Dewetting and Hydrophobic Interaction in Physical and Biological Systems. *Annu. Rev. Phys. Chem.* **2009**, *60*, 85–103.
- (11) Giovambattista, N.; Debenedetti, P. G.; Rossky, P. J. Enhanced Surface Hydrophobicity by Coupling of Surface Polarity and Topography. *Proc. Natl. Acad. Sci. U.S.A.* **2009**, *106* (36), 15181–15185.
- (12) Hummer, G.; Garde, S.; Garcia, A. E.; Pohorille, A.; Pratt, L. R. An Information Theory Model of Hydrophobic Interactions. *Proc. Natl. Acad. Sci. U.S.A.* **1996**, *93* (17), 8951–8955.
- (13) Lum, K.; Chandler, D.; Weeks, J. D. Hydrophobicity at Small and Large Length Scales. *J. Phys. Chem. B* **1999**, *103* (22), 4570–4577.
- (14) Huang, D. M.; Geissler, P. L.; Chandler, D. Scaling of Hydrophobic Solvation Free Energies. *J. Phys. Chem. B* **2001**, *105* (28), 6704–6709.
- (15) Rajamani, S.; Truskett, T. M.; Garde, S. Hydrophobic Hydration from Small to Large Lengthscales: Understanding and Manipulating the Crossover. *Proc. Natl. Acad. Sci. U.S.A.* **2005**, *102* (27), 9475–9480.
- (16) Mittal, J.; Hummer, G. Static and Dynamic Correlations in Water at Hydrophobic Interfaces. *Proc. Natl. Acad. Sci. U.S.A.* **2008**, *105* (51), 20130–20135.
- (17) Patel, A. J.; Varilly, P.; Chandler, D. Fluctuations of Water near Extended Hydrophobic and Hydrophilic Surfaces. *J. Phys. Chem. B* **2010**, *114* (4), 1632–1637.
- (18) Godawat, R.; Jamadagni, S. N.; Garde, S. Characterizing Hydrophobicity of Interfaces by Using Cavity Formation, Solute Binding, and Water Correlations. *Proc. Natl. Acad. Sci. U.S.A.* **2009**, *106* (36), 15119–15124.
- (19) Pohorille, A.; Wilson, M. A. Molecular-Structure of Aqueous Interfaces. *Theochem-Journal of Molecular Structure* **1993**, *103* (3), 271–298.
- (20) Sarupria, S.; Garde, S. Quantifying Water Density Fluctuations and Compressibility of Hydration Shells of Hydrophobic Solutes and Proteins. *Phys. Rev. Lett.* **2009**, *103* (3), 037803.
- (21) Pratt, L. R.; Chandler, D. Hydrophobic Interactions and Osmotic 2nd Virial-Coefficients for Methanol in Water. *J. Solution Chem.* **1980**, *9* (1), 1–17.
- (22) Ben-Naim, A. *Molecular Theory of Water and Aqueous Solutions* World Scientific; 2009.
- (23) Choudhury, N.; Pettitt, B. M. The Dewetting Transition and the Hydrophobic Effect. *J. Am. Chem. Soc.* **2007**, *129* (15), 4847–4852.
- (24) Chandler, D.; Weeks, J. D.; Andersen, H. C. Van Der Waals Picture of Liquids, Solids, and Phase-Transformations. *Science* **1983**, *220* (4599), 787–794.
- (25) Berendsen, H. J. C.; Grigera, J. R.; Straatsma, T. P. The Missing Term in Effective Pair Potentials. *J. Phys. Chem.* **1987**, *91* (24), 6269–6271.
- (26) Nose, S. J. A Unified Formulation of the Constant Temperature Molecular Dynamics Method. *J. Chem. Phys.* **1984**, *81*, 511–519.
- (27) Hoover, W. G. Canonical Dynamics: Equilibrium Phase-Space Distribution. *Phys. Rev. A* **1985**, *31*, 1695–1697.
- (28) Parrinello, M.; Rahman, A. Polymorphic Transitions in Single Crystals: A New Molecular Dynamics Method. *J. Appl. Phys.* **1981**, *52*, 7182–7190.
- (29) Essmann, U.; Perera, L.; Berkowitz, M. L.; Darden, T.; Lee, H.; Pedersen, L. G. A Smooth Particle Mesh Ewald Method. *J. Chem. Phys.* **1995**, *103* (19), 8577–8593.
- (30) Lindahl, E.; Hess, B.; van der Spoel, D. Gromacs 3.0: A Package for Molecular Simulation and Trajectory Analysis. *J. Mol. Model.* **2001**, *7*, 306–317.

JP1072654